Supporting information

Simultaneous top and bottom perovskite interface engineering by fullerene surface modification of titanium dioxide as electron transport layer

John Ciro, Santiago Mesa, Juan Felipe Montoya, José Ignacio Uribe, Rafael Betancur and Franklin Jaramillo[*]

Centro de Investigación, Innovación y Desarrollo de Materiales – CIDEMAT, Facultad de Ingeniería, Universidad de Antioquia UdeA, Calle 70 No. 52-21, Medellín, Colombia.

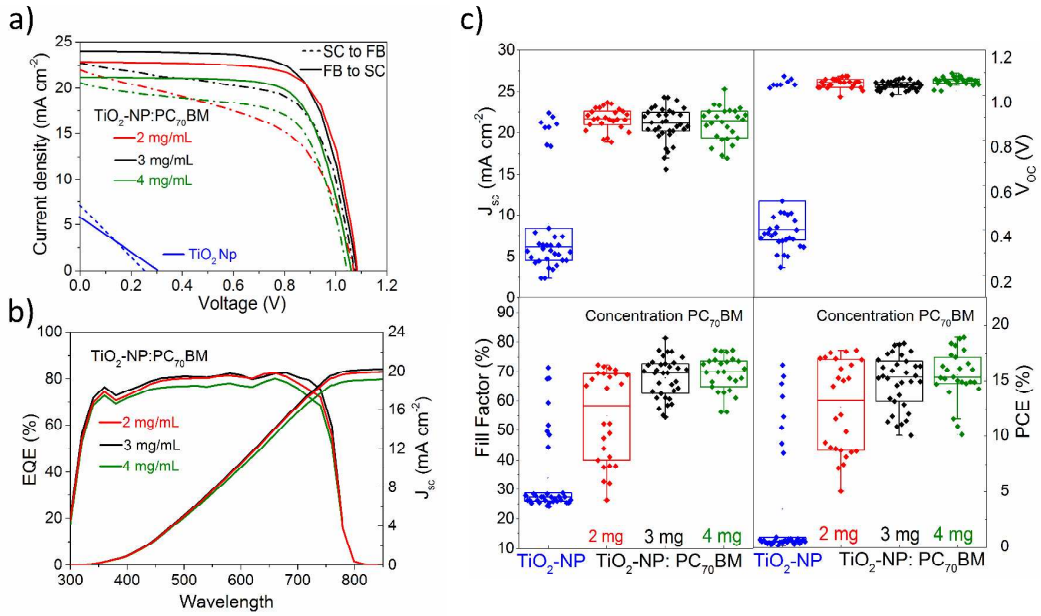

Figure S1. (a) Dependence of the resulting photovoltaic performance on the concentration of the $PC_{70}BM$ solution employed to modify the TiO_2-NP layer. (b) Corresponding EQE and (c) Statistical dispersion of the obtained photovoltaic parameters.

Corresponding Author *E-mail: franklin.jaramillo@udea.edu.co

Table S1. Photovoltaic parameters of the optimized solar cell devices depending on the $PC_{70}BM$ concentration. Best values achieved are presented in parenthesis. Average values correspond to 16 devices.

[$PC_{70}BM$] (mg/mL)	Scan direction	Jsc (mA/cm^2)	V_{oc} (V)	FF (%)	PCE (%)
2	FB to SC	22.46 ± 0.86	1.07 ± 0.01	69.07 ± 2.36	16.62 ± 0.98 (17.68)
	SC to FB	20.90 ± 1.25	1.04 ± 0.02	42.54 ± 10.04	9.23 ± 2.30 (11.93)
3	FB to SC	21.82 ± 1.58	1.05 ± 0.02	72.98 ± 4.36	16.69 ± 1.21 (18.39)
	SC to FB	20.22 ± 2.20	1.05 ± 0.02	69.21 ± 5.94	15.08 ± 1.25 (15.27)
4	FB to SC	21.08 ± 1.79	1.07 ± 0.02	71.60 ± 5.85	16.11 ± 2.33 (18.78)
	SC to FB	21.02 ± 2.28	1.06 ± 0.01	67.22 ± 6.03	14.95 ± 2.04 (15.20)
0 (Bare TiO_2)	FB to SC	13.78 ± 8.27	0.80 ± 0.33	44.10 ± 17.42	6.23 ± 6.47 (16.45)
	SC to FB	5.79 ± 1.65	0.38 ± 0.07	26.59 ± 1.14	0.52 ± 0.16 (0.76)

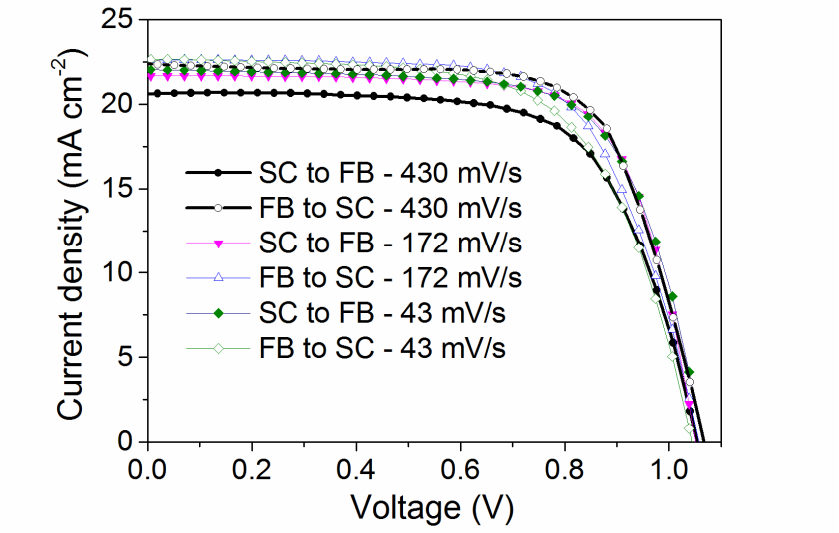

Figure S2. J-V curves of devices measured (concentration of $PC_{70}BM$: 3 mg/mL) at different scan rates (43, 172 and 430 mV/s).

The table S2 Show the corresponding device parameters at different scan rates. The hysteresis has been quantified by calculating the hysteresis index (HI) as follows[1]:

$$\mathbf{HI} = \frac{J_{FB\ to\ SC}\left(\frac{V_{OC}}{2}\right) - J_{SC\ to\ FB}\left(\frac{V_{OC}}{2}\right)}{J_{FB\ to\ SC}\left(\frac{V_{OC}}{2}\right)}$$

Where $J_{FB\ to\ SC}$ and $J_{SC\ to\ FB}$ are the currents when half of the V_{oc} voltage is applied for reverse (from V_{oc} to zero) and for forward (from zero to V_{oc}) voltage scans, respectively. A device without hysteresis presents a HI of zero, while higher values of HI indicate a more hysteresis. When we scan rates more slow, the HI is gradually reduced.

Table S2. The corresponding device parameters at different scan rates (43, 172 and 430 mV/s) and the quantified of its hysteresis.

Scan direction	Jsc (mA/cm^2)	V_{oc} (V)	FF (%)	PCE (%)	HI
FB to SC - 430 mV/s	22.39	1.07	68.52	16.46	0.100
SC to FB - 430 mV/s	20.60	1.04	68.54	14.69	
FB to SC - 172 mV/s	22.02	1.07	69.47	17.13	0.066
SC to FB - 172 mV/s	22.65	1.04	65.46	16.09	
FB to SC - 43 mV/s	21.68	1.07	70.87	16.41	0.020
SC to FB - 43 mV/s	22.50	1.07	66.28	15.97	

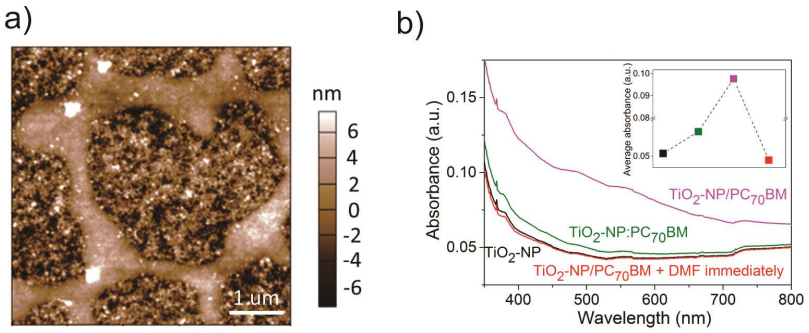

c)

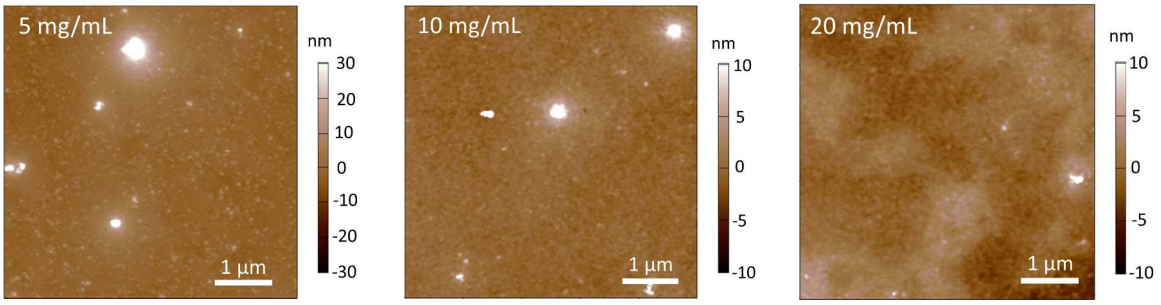

Figure S3. (a) Topography of TiO_2-NP:$PC_{70}BM$ layer. (b) Optical absorption of the TiO_2-NP (black line) layer and the TiO_2-NP/$PC_{70}BM$ (magenta line) bilayer. The interaction of the TiO_2-NP/$PC_{70}BM$ bilayer with DMF was evaluated to corroborate if $PC_{70}BM$ remains after depositing the perovskite. After 12 hours, $PC_{70}BM$ is physisorbed to the TiO_2-NP and it is not fully removed by DMF (green line). In contrast, $PC_{70}BM$ is fully removed when DMF is dripped immediately after the $PC_{70}BM$ layer deposition (red line). Inset: Corresponding average absorbance in the 350-700 nm range. (c) Topography of TiO_2-NP:$PC_{70}BM$ layers grown from precursor with solid concentration up to 20 mg/mL

Depositing $PC_{70}BM$ on top of TiO_2-NP strongly enhanced the optical absorption between 350 and 700 nm (magenta and black lines in Figure S3, respectively). The $PC_{70}BM$ layer was fully removed when the substrate interacted with DMF immediately after the $PC_{70}BM$ deposition (red line). For that reason, the $PC_{70}BM$ was allowed to interact with the np-TiO_2 layer during 12 hours before depositing the perovskite. In that case, the $PC_{70}BM$ remained presumably physisobed as evidenced by the green line in Figure S3.

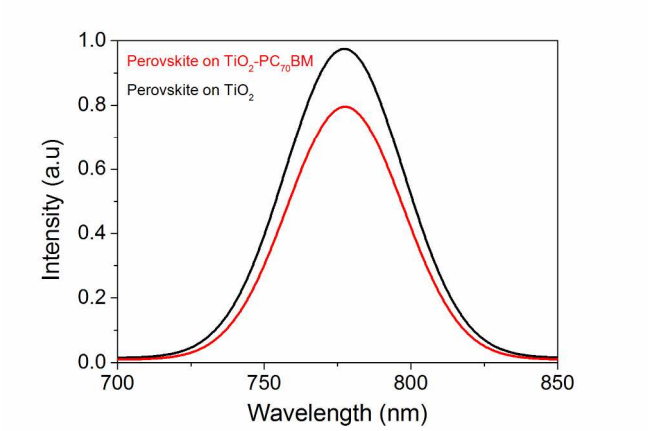

Figure S4. Steady-state photoluminescence (PL) spectra of the perovskite on TiO_2-NP and TiO_2-NP:$PC_{70}BM$.

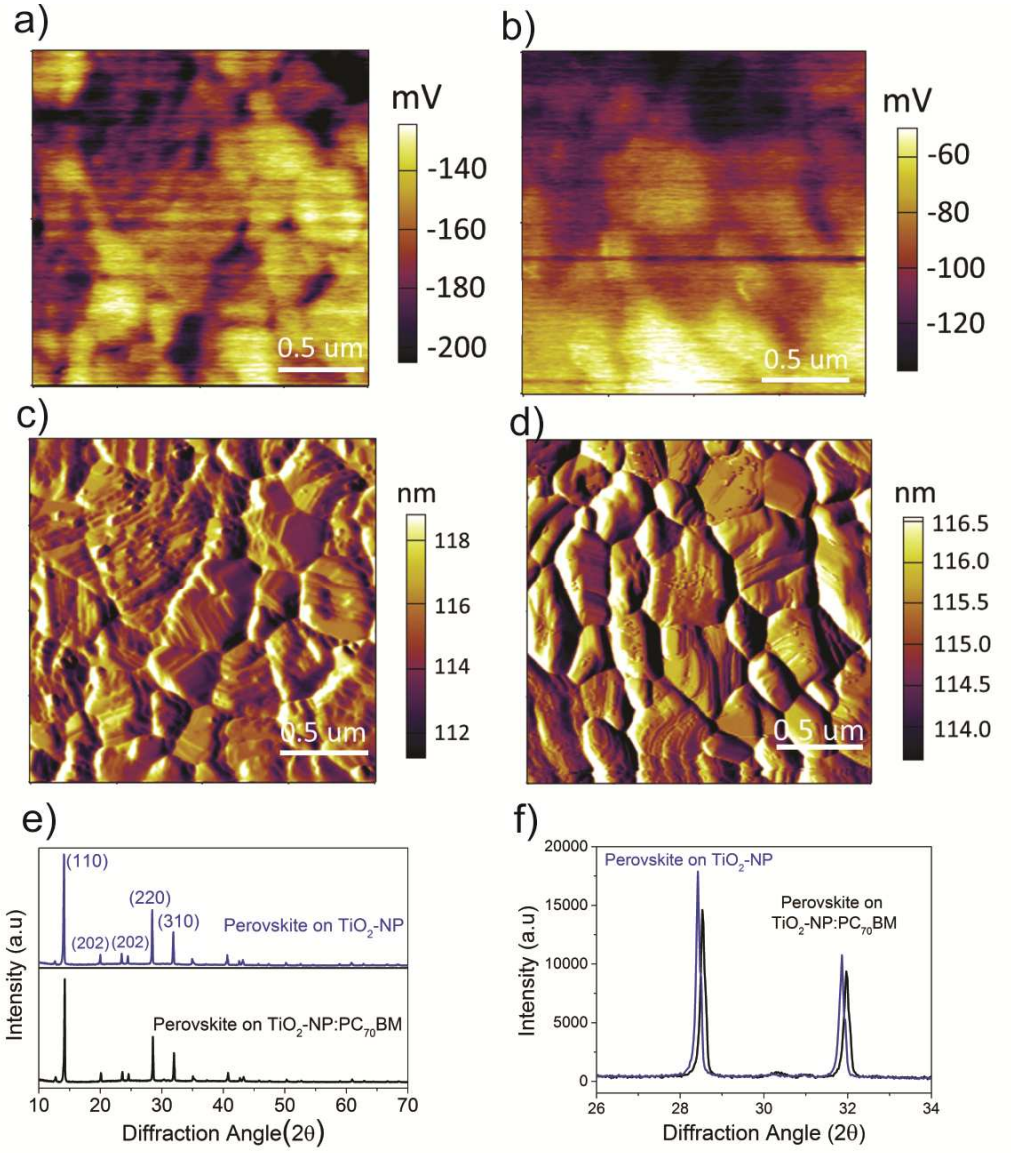

Figure S5. Electronic and morphologic properties of the grown perovskite depending on the underlying ETL. Contact voltage and retrace amplitude of the perovskite deposited on (a), (c) TiO_2-NP:$PC_{70}BM$ layer and (b), (d) TiO_2-NP layer. (e) Difractogram of the perovskite. (f) Zoom of the overlaid difractograms.

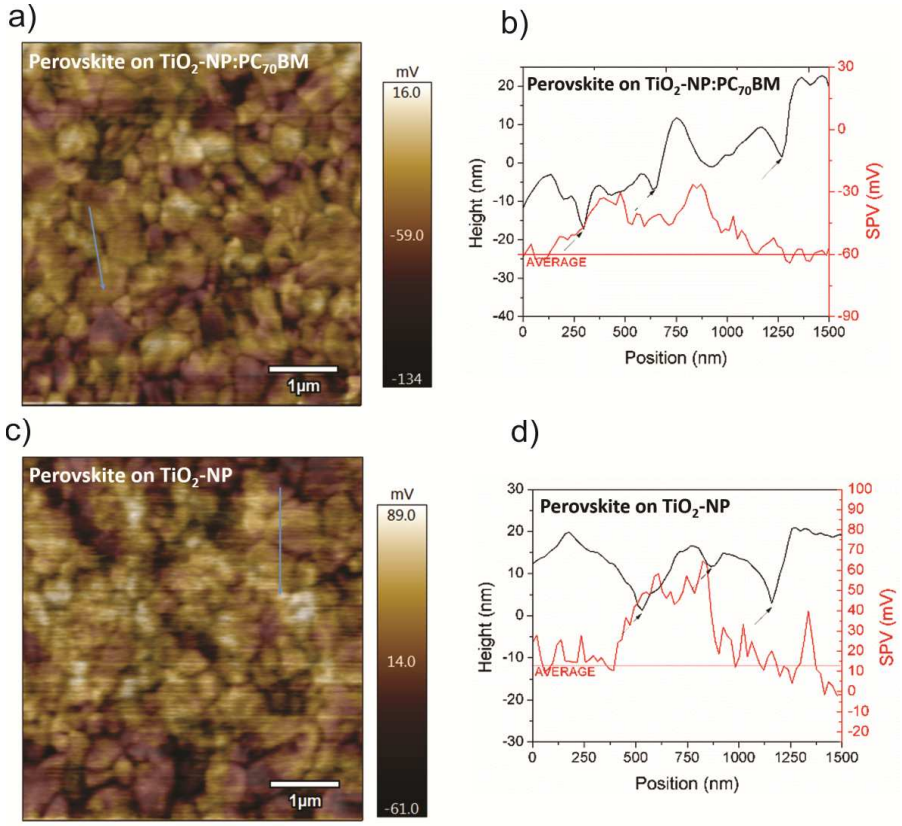

Figure S6. Overlaid SPV and topography maps and profiles for the perovskite grown on (a), (b) TiO_2-NP:$PC_{70}BM$ and (c), (d) TiO_2-NP layers, respectively.

References

(1) Sanchez, R. S.; Gonzalez-pedro, V.; Lee, J.; Park, N.; Kang, Y. S.; Mora-sero, I.; Bisquert, J. Slow Dynamic Processes in Lead Halide Perovskite Solar Cells. Characteristic Times and Hysteresis. *J. Phys. Chem. Lett.* **2014**, 2357–2363.